BOILING HEAT TRANSFER INSIDE PARALLEL MICROCHANNELS

Evandro Rodrigo Dario[a], Júlio César Passos[b]*, María Luisa Sánchez Simón[c], and Lounès Tadrist[d]
*Author for correspondence
[a] Federal Institut of Santa Catarina, Joinville-SC, Brazil
[b] Department of Mechanical Engineering, LEPTEN, Centre of Technology,
Federal University of Santa Catarina, Florianópolis-SC, 88040-900, Brazil; E-mail: julio.passos@ufsc.br

[c] Sistemas Térmicos y Transferencia de Calor, Departamento de Enxeñaría Naval e Oceánica, Escola Politécnica Superior, Universidade da Coruña, Campus de Ferrol, 15471 Ferrol, Spain

[d] Aix-Marseille Université, CNRS, IUSTI UMR 7343, 13013 Marseille, France

ABSTRACT

Heat transfer study was carried out on convective boiling of R134a through nine horizontally positioned, parallel microchannels. The microchannels were of circular cross sections with internal diameter and length of 0.77 mm and 150 mm, respectively. The test conditions are as follows: mass velocity, G, of 250, 500, 750 and 1000 kg/m^{2}s; inlet pressure, p_{in}, of 600, 700, and 900 kPa and subcooling degrees of 1, 10 and 20^{o}C. The experimental results for heat transfer coefficient are compared with seven correlations and semi-empirical models and the best predictions are obtained with the models of Sun and Mishima [13] and Thome et al. [15] for which the Mean Absolute Error was 14.4% and 14.9%, respectively.

INTRODUCTION

Boiling heat transfer is present in many industrial applications. The search for compactness and miniaturization of heat exchangers became the main motivation for continuous studies on flow boiling in microchannels which hydraulic diameter is lower than or close to the millimeter. Indeed, the ratio of heat transfer area and volume for a tube is inversely proportional to the diameter and increases as the diameter decreases. Because flow boiling in microchannels can present high heat flux it is considered as an attractive process for cooling electronic devices [1].

Recently, an increase number of studies focused on two-phase flow boiling of refrigerant R134a and new refrigerants inside a copper multi-microchannel heat sink for microelectronic central processing unit cooling applications.

With the existence of a great number of boiling flow studies inside microchannels, and due to the difficulty of visualizing diabatic flows, some authors showed that flow maps for isothermal two-phase flow, in general using air and water, can be carefully applied to the microchannel exchangers. Revellin et al. [2] determined the two-phase flow of R134a characteristics at the exit of an evaporator microchannel of 0.5 mm diameter, by means of an optical method consisted of two laser beams, and observed four principal flow patterns and two intermediate transition regimes. By this method three principal flow patterns were identified: bubbly, slug and annular flows. The fourth flow pattern is the dryout regime which represents a necessary point for the design of heat exchangers as miniaturized evaporators. In parallel microchannels evaporators the dryout heat flux, DHF, can be influenced by the two phase flow distribution that depends on the two-phase flow pattern inside the header, [3]. This is not yet completely understood and further experiments are still necessary. Revellin et al. [2] also reported that there is important differences between the transition lines for flow boiling of R134a inside a microtube with 0.5 mm of diameter, in a plot of the liquid superficial velocity as function of the vapor superficial velocity, and those for air-water flow in a 1.097 mm tube diameter obtained by [4]. Indeed, for the diabatic cases the vapor quality increases along a heated channel. In [5], for boiling flow of R245fa in a microchannel of 0.5 mm and for the same experimental condition and quality (x=23%) wavy-annular and smooth-annular flows were observed and the transitions from slug to semi-annular flow was observed for a vapor quality x=7% whereas that one from semi-annular to wavy-annular was observed for x=23%.

Revellin and Thome, [6], propose a new type of diabatic flow pattern map for boiling heat transfer in microchannels based in a visualization study data base covering two refrigerants (R-134a and R-245fa) and two channel diameters (0.509 and 0.790 mm).

Madhour et al. [7] reported the main trends they found, using R134a as working fluid: the heat transfer coefficient increased with heat flux and was independent of the mass flow rate and the heat transfer coefficient could reach 270 kW/m^{2}K.

Agostino and Thome [8], based on the analysis of 13 studies, showed the opposite trends in the results and found as main trend, for qualities between 0.05 and 0.5, that the heat transfer coefficient, HTC, decreases with the increase of the vapour quality and increases with the heat flux. For higher vapour qualities (x > 0.5), the HTC drastically decreased with the quality and was independent of the mass velocity and heat flux, that means that the dryout condition was initiated or reached.

Ribatski et al. [9] analysed several experimental studies in the literature and also verified that authors found different trends, that in some cases are completely opposite. These

authors also remarked that several studies considered that the nucleate boiling regime was the dominant heat transfer mechanism during flow boiling in microchannels, without any proof. Jacobi and Thome [10] modelled the flow boiling for the configuration with elongated bubbles separated by liquid slugs and showed that the effect of the heat flux on the HTC can be explained by the evaporation of the thin liquid layer between the wall channel and the elongated bubble.

The above review of the literature shows that many questions during flow boiling inside parallel microchannels are still not well answered. Therefore new experimental and theoretical analysis need to be done. This study reports experimental results for the heat transfer coefficient during the inlet subcooled horizontal flow boiling of R134a inside nine parallel copper microchannels of inner diameter 0.77 mm, and 150 mm length.

NOMENCLATURE

c_p	[J/kgK]	Specific heat
d	[m]	Diameter
g	[m/s^2]	Acceleration due to gravity
G	[kg/m^{2}s]	Mass velocity
i	[J/kg]	Enthalpy
h	[kW/m^{2}K]	Heat transfer coefficient (HTC)
i_{lv}	[J/kg]	Latent heat of vaporization
L_{sub}	[m]	Subcooled length
p	[Pa]	Pressure
p_{crit}	[Pa]	Critical pressure
q”	[W/m^2]	Heat flux
T	[K]	temperature
x	[-]	Vapour quality
z	[m]	Axial position

Special Characters

Δp	[Pa]	Pressure drop
ΔT	[K]	Temperature difference
ΔT_{sub}	[K]	Subcooling degree, $\Delta T_{sub} = T_{sat} - T$
ΔTsup	[K]	Wall superheating, $\Delta T_{sup} = T_w - T_{sat}$
ρ	[kg/m^3]	Density
σ	[kg/s^2]	Surface tension

Subscripts

acc	Acceleration contribution to the pressure drop
ad	Adiabatic
cal	Calculated
exp	Measured value
in	Test section inlet
out	Test section outlet
pre	Predicted value
sat	Saturated
sp	Single-phase
sub	Subcooled
sup	Superheated

EXPERIMENT

Experimental Setup

The experimental facility designed for the study of the thermohydraulic phenomena in microchannels, obviates the problems with non uniform heating and leakage between channels. The facility comprises a main closed circuit in which the flow of refrigerant, R134a, is impelled by a magnetic gear pump through a filter, a mass flow meter, two preheaters, the test section, and a condenser. More details about the experimental setup are presented in [11 and 12].

The test section is composed of nine parallel copper micro channels, whose central section is inserted in slits machined in the inner face of two copper plates. The microchannels have an internal diameter of 0.77 ± 0.1 mm, with a roughness of 0.59 μm, and an external diameter of 2.0 mm. Their total length is 150.0 mm. The copper plates have a length of 120.0 mm, a width of 60.0 mm, and a thickness of 4.1 mm. The microchannels and the plates were carefully welded in order to ensure uniform heat conduction. Two skin resistance heaters of 12.5 Ω each, cover the external faces of the plates, and thermal grease is used to ensure a uniform heat distribution and to reduce thermal resistance. All these elements are placed between two Teflon pieces, which provide thermal insulation. The Teflon pieces are compressed between two plates of steel in order to achieve mechanical robustness, as well as a good thermal contact between the skin heaters and the copper plates. Finally, the whole ensemble is surrounded by mineral wool.

At each end of the microchannels, two plena (a distributor and a collector) ensure uniform conditions of inlet and outlet pressures and inlet temperature. These plena have an internal diameter of 20.0 mm and a length of 80.0 mm.

An important point related to the design of the test section is that there is no possibility of secondary flows or leakage between the parallel channels.

In the test section, inlet pressure as well as the pressure drop are measured by means of two pressure transducers. The inlet temperature, T_{in}, is measured by an E-type thermocouple, inserted in the inlet plenum in order to ensure a higher accuracy and faster response. The uncertainties of these variables are given in Table 1.

Temperatures in the microchannels are measured by means of 21 E-type thermocouples distributed in seven sections to ensure the uniformity of the heat flux in the test section. The uncertainty of the temperature measured by the thermocouples is ± 0.2 °C.

Experimental Conditions and Procedure

This section includes a description of the experimental conditions of the tests, and the procedure to ensure the quality of the results.

For the study of the heat transfer coefficient 1160 experiments were carried out. The values of the experimental conditions of the tests and their uncertainties are included in Table 1.

The uniformity of temperatures among the channels was verified by a numerical simulation of the heat conduction in the test section. In addition, an experimental test confirmed evenness in both temperature and flow distribution among the channels. The performance of the test section was also

evaluated by means of single-phase flow experiments. Furthermore, the reproducibility of the tests was verified. Each test was characterized by fixed values of the inlet flow conditions, namely, mass flow rate, subcooling degree, and inlet pressure. These variables were set at the beginning of the test, and kept stable for the whole duration. Small increases in the flux were applied, and data were acquired, subsequent to the stabilization of all variables.

Table 1 Experimental conditions and uncertainties.

Test defining variables	**Nominal Value**	**Uncert.**
Heat flux, q" [kW/m^2]	5–220	<3.8%
Inlet variables		
Mean mass velocity, G [kg/m^{2}s]	250, 500, 750, 1000	<0.5%
Inlet pressure, p_{in} [kPa]	600, 700, 900	<0.1 kPa
Subcooling degree, ΔT_{sub} [°C]	1, 10, 20	
Other measured variables		**Uncert.**
Temperature (TC in test section), [°C]		0.2 °C
Total pressure drop, Δp_{tot} [kPa]		<0.1 kPa
Calculated variables	**Range**	**Uncert.**
Inlet saturation temperature, $T_{in,sat}$ [°C]	21.6, 26.7, 31.5	<3.8%
Vapor quality, x [%]	0–0.95	<4.1%
Heat transfer coefficient [kW/m^{2}K]		
$Re_{l,in}$	< 500	
Bo_{in}		

Of the 150 mm total length of the microchannels, heat flux was applied only to the central 120 mm portion. It was assumed that the initial and final sections were adiabatic. Thus, at the beginning of the diabatic portion, the flow was subcooled for a length L_{sub}. The subcooled length was determined by an iterative procedure, in which the liquid temperature obtained from an energy balance,

$$T_{sp}(z) = \frac{q''}{G c_p}\frac{4\,z}{d} + T_{in}, \quad (1)$$

was compared to the saturation pressure corresponding to the local pressure,

$$T_{sat} = f(p). \quad (2)$$

The local pressure, in turn, was obtained from the inlet pressure, p_{in}, and the single-phase pressure drop Δp_{sp} assessed by the equations for pressure losses in laminar or turbulent flow.

$$p_{sat}(z) = p_{in} - \Delta p_{sp}(z)\,, \quad (3)$$

In equation (1) q'' represents the heat flux imposed on the test section, which is obtained from the electric power supplied; G is the mass velocity; c_p is the specific heat of the refrigerant; d denotes the channel diameter; and T_{in} is the inlet temperature.

The subcooled length, L_{sub}, represents the location of the section where the thermodynamic equilibrium quality is zero. However, at this region the real quality is not zero. Neglecting real vapour quality until at z= L_{sub} the quality is determined by the following energy balance equation:

$$x = \frac{1}{i_{lv}(z)}\left\{\frac{q''}{G}\frac{4}{d}(z - L_{sub}) + c_p(\mathrm{z})\,[T_{sat}(\mathrm{z}) - T_{sat}(L_{sub})\right\}. \quad (4)$$

The saturated temperature was obtained from the local pressure, which, here, is assumed to vary linearly from L_{sub} to the position considered. This approximation was made in view of the low values of the total pressure drop measured.

The measured temperatures, at a given cross section, were averaged and the heat transfer coefficient is calculated by means the following equation:

$$h_z = \frac{\overline{q''}}{T_{w,i}(z) - T_{sat}(z)}\,, \quad (5)$$

where $\overline{q''}$ is the average heat flux, in kW/m^2 and $T_{w,i}(z)$ is the extrapolated temperature of the inside surface of the channel, at z.

RESULTS AND DISCUSSION

Experimental Heat Transfer Coefficient

Figure shows the evolution of the local heat transfer coefficient with local vapour quality for various values of the heat flux, for inlet pressure p_{in}=700 kPa, subcooling degree ΔT_{sub}=1.1 K, and mass velocity G=1002 kg/m^{2}s. As observed, heat transfer coefficient (HTC) strongly depends on heat flux. Regarding the influence of vapour quality, in the range of low quality x, *HTC* have their maximum values and decrease rapidly, whereas for intermediate vapour qualities *HTC* are nearly constant, around 80% of their maximum value. For higher heat fluxes (160 and 210 kW/m^2) and qualities higher than 0.5 the HTC decreases with quality. These results agree with the main trend of published results as seen in the introduction. This trend for the beginning of the dryout agrees well with the prediction in the flow pattern map proposed in [6].

Figure 2 shows the influence of mass velocity for a heat flux of 120 kW/m^2, inlet pressure of 700 kPa (T_{sat}= 26.7 ºC), and low inlet subcooling of 1 K. The HTC is almost independent of mass velocities between 500 and 1000 kg/m^{2}s. After a certain value of the quality the HTC becomes constant.

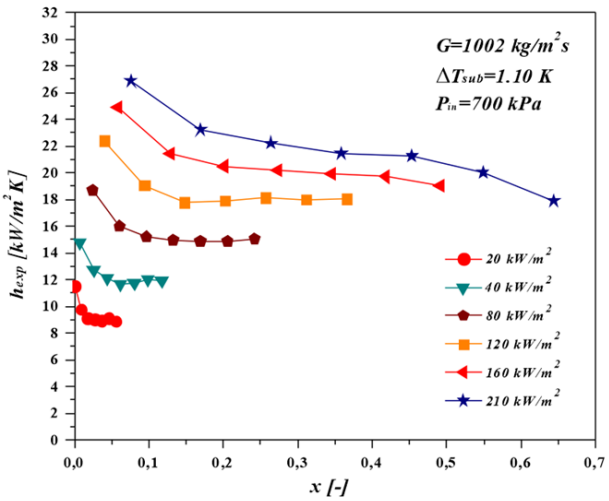

Figure 1 Influence of heat flux on the local heat transfer coefficient.

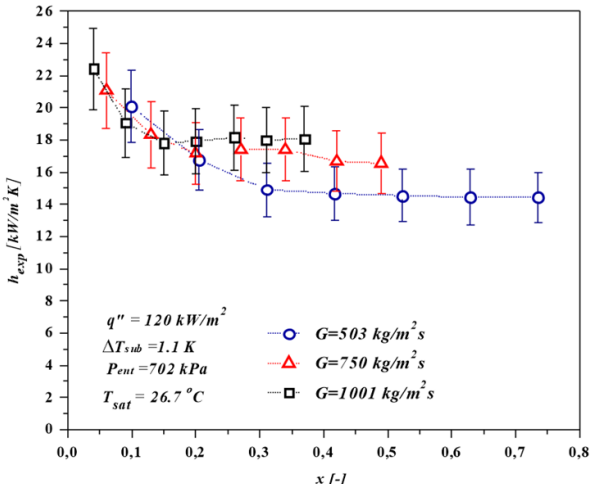

Figure 2 Influence of mass velocity on local heat transfer coefficient. Nominal inlet pressure p_{in}= 700 kPa, T_{sat}= 26.7 ºC, ΔT_{sub}= 1.1 K, q''= 120 kW/m^2.

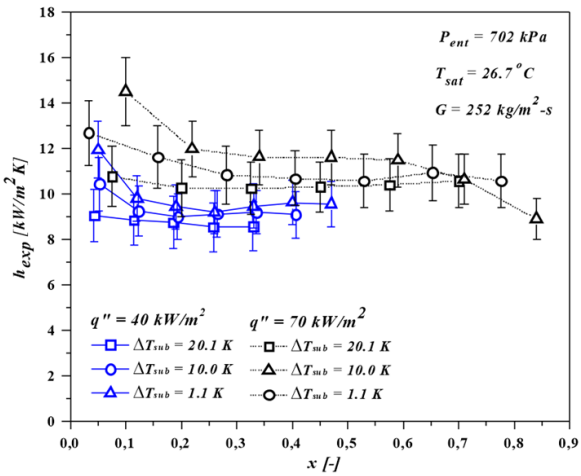

Figure 3 Influence subcooling degree on local heat transfer coefficient for two values of the heat flux of q''= 40 kW/m^2 and q''= 70 kW/m^2. Nominal mass velocity G= 250 kg/m^{2}s, p_{in}= 700 kPa, T_{sat}= 26.7 ºC.

Taking into consideration the results of the last figure, an attempt to relate the evolution of the *HTC* with the flow pattern can be done considering the Revellin and Thome [6] map. Similar to what happens in conventional channels, in the range of low vapor qualities the HTC is unaffected by mass velocity. That is a trend similar to that one during nucleate boiling and when the regime is the isolated bubble (*IB*). The *(IB)* regime, [6], is characterized "by a bubble generation rate much larger than the bubble coalescence rate" and can include both bubbly flow or/and slug flow or coalesced bubbles (*CB*).

For increasing qualities, the decreasing values of the HTC, which is affected by mass velocity, can be attributed to a confined bubble regime (CB). In this regime, the heat transfer is governed by the cyclic evaporation of the thin liquid layer between the bubble and the wall, and by the flow of the liquid portions between consecutive bubbles, thus making convective boiling the prevailing mechanism. The value of the HTC was expected to increase with quality associated to the annular (*A*) regime, since the decrease of the liquid layer thickness leads to a lower thermal heat transfer resistance, enhancing the convective transport of heat across the film. In fact, the average values for HTC are almost constant in the annular flow. Finally, for higher qualities, the HTC decreases in the dryout region. This behaviour agrees well with the flow map presented by Revellin and Thome [6] for mass velocities higher than 503 kg/m^{2}s. However this is not the case for low mass velocities, as for example, equal to 252 kg/m^{2}s, when the dryout starts for a quality higher than 60% whereas the flow map of [6] predicts this for quality higher than 90%.

Figure 3 illustrates the influence of subcooling degree and compares the evolution of HTC with quality for values of the heat flux of 40 and 70 kW/m^2, and for nominal inlet subcooling degrees, ΔTsub, of 1.0, 10.0 and 20.0 K. In the evolution of HTC with vapour quality, two behaviours can be observed. For lower qualities, the heat transfer coefficient is influenced by the subcooling degree, decreasing with it. Moreover, the decrease of the HTC with quality is less pronounced when the subcooling increases. A different trend is observed for higher qualities. The HTC tends to a nearly constant value, independent of the subcooling. The value of the local vapour quality in which the trend changes increases with heat flux.

In the low quality range , i.e. for positions which are closer to the subcooled region, the bulk liquid is subcooled for a length downstream of the axial position L_{sub}, where the thermodynamic quality is equal to zero. The subcooling degree is one of the parameters that influences the range of active cavities in the model of Hsu [13]. A decrease of the subcooling increases the range of active cavities; moreover a lower wall superheating is needed to activate them. Thus, lower subcooling degrees enhance nucleate boiling and lead to higher values of the HTC. For higher qualities all liquid is saturated and convective boiling takes control, and therefore the subcooling degree does not influence the heat transfer process.

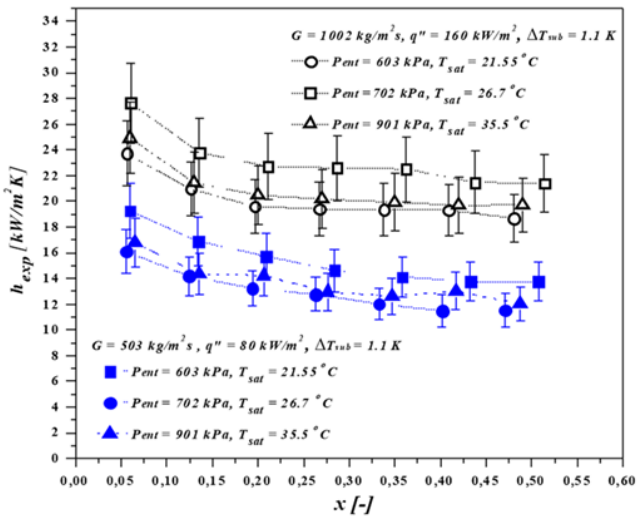

Figure 4 Influence saturation temperature degree on local heat transfer coefficient for two values G and q´´. p_{in}= 700 kPa, ΔT_{sub}= 1.1 K.

Figure 4 compares the *HTC* for subcooling degree, ΔT_{sub}= 1.1K, for three different values of the saturation temperature, T_{sat}, of 21.5 ºC, 26.7 ºC and 35.5 ºC and for two conditions of mass velocity and heat flux, keeping the boiling Number constant *Bo*= 9.09x10^{-4}. These conditions are of nominal mass velocity of 500 kg/m^{2}s and q''= 80 kW/m^2, and *G*= 1000 kg/m^{2}s and q''= 160 kW/m^2. An increase of HTC with saturation temperature, independently of mass velocity or quality is observed analogously to conventional channels. Moreover, the effect of saturation temperature increases with heat flux. These trends can be explained by the enhancement of the heat transfer with saturation temperature.

It is necessary to note, that the increase of saturation temperature increases the wall temperature T_w, via an enhancement of heat transfer, which causes a decrease of the wall superheating $\Delta T_{sup}= T_w-T_{sat}$.

Comparison with models and correlations

The present results are used to assess the performance of the seven models and correlations for the HTC found in the literature and shown in Table 2**.** A statistical performance is assessed by means of two parameters: the Mean Absolute Error (MAE) and the percentage of date within deviations of ± 20% and ± 30%. The MAE is calculated from Eq. 6,

$$MAE(\%) = \frac{100}{N}\sum_{i=1}^{N}\left|\frac{h_{exp\ i}-h_{pre\ i}}{h_{exp\ i}}\right|, \qquad (6)$$

where $h_{exp,i}$ e $h_{pre,i}$ are the experimental and the corresponding predicted value, respectively.

Table 2 summarizes the performance of the correlations for the present 1,160 point database. The values of the MAE and the number of points whose deviation falls within the ranges of ± 30% and ± 20% are also provided.

Table 2 Predictions of the HTC with different correlations and models for the present database.

Correlation/model	**MAE**	**±30%**	**±20%**
Sun and Mishima [14]	14.4 %	93.3 %	74.9 %
Lazarek and Black [15]	23.2 %	67.4 %	49.0 %
Thome et al. [16]	14.9 %	90.8 %	73.2 %
Tran et al. [17]	48.4%	3.5%	-
Yu et al. [18]	18.2 %	81.9 %	62.5 %
Kew and Cornwell [19]	27.8 %	59.9 %	-
Kandlikar and Balasubramanian [20]	37.5 %	37.2 %	-

It's interesting to verify the ability of these correlations for capturing the trends in the evolution of the experimental results. In Figure 5 the evolution with quality of the experimental and predicted values of the HTC are compared for the condition of nominal mass flow rate and inlet pressure of G=500 kg/m^{2}s and p_{in}= 700 kPa, saturation temperature of 26.7 ºC, and subcooling degree of ΔT_{sub}= 1.1 K.

According to Table 2, the best prediction corresponds to the correlation of Sun and Mishima [14] with a MAE of 14.4 %

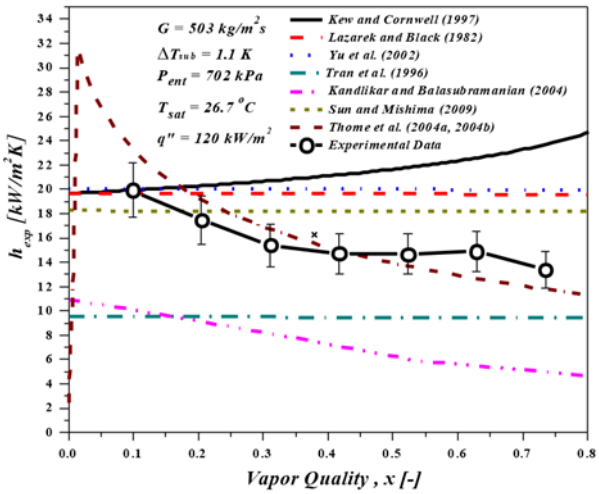

Figure 5 Comparison of experimental and predicted values of HTC as a function of vapour quality. G= 500 kg/m^{2}s, p_{in}= 702 kPa, T_{sat}= 26.7 ºC, ΔT_{sub}= 1.1 K

and with 93.3% of points within a 30% of deviation. This correlation is based on the correlation of Lazarek and Black [15] and incorporates a large database with an important presence of measurements of R134a in microchannels. However, this correlation does not predict the trend of the experimental HTC vs vapour quality, as observed in Figure 5.

The model of Thome et al. [16] performs well with a MAE of 14.9% and 90.8 % of points within a deviation of ±30%. Moreover, this model is able to predict satisfactorily the evolution of HTC vs quality, and despite the fact that it was derived for the Confined Bubble regime, this method leads to good results also in the annular regime as pointed out by Chen et al. [18].

Although developed for a data base which does not include R134a, and for channels with diameters larger than one used in the present study, the correlations of Yu et al. [19] and Lazarek and Black [15] perform almost satisfactorily with a MAE below 25%. Nevertheless, these correlations fail in predicting the evolution of the HTC with quality.

The correlation of Kew et al. [12], based on results for R141b in the range of diameters of 1.39 to 3.69 mm performs well with a MAE of 27.8% but is unable to predict the evolution of the HTC with quality.

The correlation of Kandlikar et al. [13] was obtained from a large database that includes R134a and a wide range of diameters, which include the present one. Even though, it presents a MAE of only a 37.53%, this correlation predicts satisfactorily the trend in the evolution of the heat transfer coefficient with quality.

CONCLUSIONS

An experimental study on flow boiling of the R134a inside nine horizontal parallel microchannels of an internal diameter of 0.77 ± 0.1 mm and a heated length of 120 mm was performed. The following results can be drawn:

The heat transfer coefficient strongly was found to depend on heat flux and increases with it, which agrees with the main trend of published results.

The HTC is almost independent of mass velocities between 500 and 1000 kg/m^{2}s. After a certain value of the quality the HTC becomes constant.

The HTC is more influenced by the subcooling degree in the low vapour quality region. For higher qualities it tends to a nearly constant value, independent of the subcooling.

The HTC increases with the saturation temperature, but is independent of the mass velocity or quality and the effect of saturation temperature increases with heat flux.

For higher qualities, the HTC decreases in the dryout region, agreeing with the flow map of [6] for mass velocities higher than 503 kg/m^{2}s. For low mass velocity, as 252 kg/m^{2}s for example, the dryout started earlier than predicted in [6].

The best agreement between experimental and predicted HTC values was obtained by the correlations of Sun and Mishima [14] and Thome et al. [16] with values of MAE of 14.4 % and 14.9%, respectively. However, the model proposed by Thome et al. [16] was able to predict satisfactorily the evolution of HTC as function of the vapour quality.

ACKNOWLEDGEMENTS

The authors gratefully acknowledge support of this work by the Brazilian National Council of Research (CNPq), by CAPES/Brazilian Ministry of Education and the IUSTI of Aix-Marseille University. The author MLSS also thanks the Universidade da Coruña for the support under the Axudas á investigación 2014 program. The authors also thank the comments and suggestions of the reviewers.

REFERENCES

[1] Kandlikar, S.G., 2005, High flux heat removal with microchannels: a roadmap of challenges and opportunities, Heat Transfer Engineering, Taylor & Francis Inc., 26(8) (2005) 5–14.

[2] Revellin, R., Dupont, V., Ursenbacher, T., Thome, J.R., Zun, I., Characterization of diabatic two-phase flows in microchannels: flow parameter results for R134a in a 0.5mm channel, International Journal of Multiphase Flow, 32 (2006) 755-774.

[3] Dario E.R., Tadrist, L., Passos J.C., Review on two-phase flow distribution in parallel channels with macro and micro hydraulic diameters: Main results, analyses, trends, Applied Thermal Engineering, 59 (1-2) (2013) 316-335.

[4] Triplett, K., Ghiaasiaan, S., Abdel-Khalik, S.I., Sadowski, D.L., Gas-liquid two-phase flow in microchannels-Part 1: two-phase flow patterns, International Journal of Multiphase Flow, 25 (1999) 377-394.

[5] Revellin, R. and Thome, J.R., Experimental investigation of R-134a and R-245fa two-phase flow in microchannels for different flow conditions, International Journal of Heat and Fluid Flow, 28 (2007) 63-71.

[6] Revellin, R. and Thome, J.R., A new type of diabatic flow pattern map for boiling heat transfer in microchannels, J. Micromechanics and Microengineering. 17 (2007) 788–796.

[7] Madhour, Y., Olivier, J., Costa-Patry, E., Paredes, P., Michel, B., Thome, J.R., Flow Boiling of R134a in a Multi-Microchannel Heat Sink With Hotspot Heaters for Energy-Efficient Microelectronic CPU Cooling Applications, 2012.

[8] Agostino, B. and Thome, J.R., Comparison of an extended database of flow boiling heat transfer coefficient in multi-microchannel elements with the three-zone model, ECI International Conference on Heat Transfer and Fluid Flow in Microscale, Castelvecchio Pascoli, Italy, 2005.

[9] Ribatski, G., Wojtan, L., Thome, J.R., An analysis of experimental data and prediction methods for two-phase frictional pressure drop and flow boiling heat transfer in micro-scale channels, Experimental Thermal and Fluid Science 31 (2006) 1–19.

[10] Jacobi, A.M. and Thome, J.R., Heat transfer model for evaporation of elongated bubble flows in microchannels, Journal of Heat Transfer, ASME, 124 (2002) 1131-1136.

[11] Dario, E.R., Convective boiling of R134a in parallel microchannels and analysis of the air-water two-flow maldistribution inside a manifold connected to microchannels, PhD thesis, Graduate Program of Mechaanical Engineering in coorientation of Federal University of Santa Catarina, Brazil, and Aix-Marseille University, France, in Portuguese, 309 p, 2013.

[12] Dario, E.R., Passos, J.C., Sánchez Simón, M.L., Tadrist, L., Pressure drop during flow boiling inside parallel microchannels, manuscript under the final review process of the International Journal of Refrigeration, 10 p., 2016.

[13] Hsu, Y., On the size range of active nucleation cavities on a heating surface, Journal of Heat Transfer, ASME, 84(3) (1962) 207-213.

[14] Sun, L., Mishima, K. Evaluation analysis of prediction methods for two-phase flow pressure drop in mini-channels, Int. J. Multiph. Flow. 35 (2009) 47–54.

[15] Lazarek, G.M., Black, S.H., Evaporative heat transfer, pressure drop and critical heat flux in a small vertical tube with R-113, Int. J. Heat Mass Transf. 25 (1982) 945–960.

[16] Thome, J.R., Dupont, V. and Jacobi, M., Heat transfer model for evaporation in microchannels. Part I: presentation of the model, Int. J. Heat Mass Transf. 47 (2004) 3375-3385.

[17] Tran, T.N., Wambsganss, M.W., France, D.M., Small circular and rectangular channel boiling with two refrigerants, International Journal of Multiphase Flow, 22 (3) (1996) 485-498.

[18] Chen, L., Tian, Y.S. and Karayiannis, T.G., The effect of tube diameter on vertical two-phase flow regimes in small tubes, Int. J. Heat Mass Transf. 49 (2006) 4220–4230.

[19] Yu, W., France, D.M., Wambsganss, M.W. and Hull, J.R., Two-phase pressure drop, boiling heat transfer, and critical heat flux to water in a small-diameter horizontal tube, Int. J. Multiph. Flow. 28 (2002) 927–941.

[20] Kew, P., Cornwell, K., Correlations for the prediction of boiling heat transfer in small-diameter channels, Appl. Therm. Eng. 17 (1997) 705–715.

[21] S.G. Kandlikar, P. Balasubramanian, An Extension of the Flow Boiling Correlation to Transition, Laminar, and Deep Laminar Flows in Minichannels and Microchannels, Heat Transf. Eng. 25 (2004) 86–93.